[해설논문] 한국재료학회지
Korean J. Mater. Res.
Vol. 32, No. 11 (2022)

https://doi.org/10.3740/MRSK.2022.32.11.449

Recent Progress in Blue Perovskite LEDs

Joonyun Kim, Jinu Park, and Byungha Shin†

Department of Materials Science and Engineering, Korea Advanced Institute of Science and Technology, Daejeon 34141, Republic of Korea

(Received September 16, 2022 : Revised October 13, 2022 : Accepted October 20, 2022)

Abstract Halide perovskites are emerging materials for next-generation display applications, thanks to their narrow emission linewidth and band gap tunability, capable of covering the entire range of visible light. Despite their short period of research, perovskite light emitting diodes (PeLEDs) have shown rapid progress in device external quantum efficiency (EQE) in the near-infrared (NIR), red, and green emission wavelengths, and the record EQE has exceeded over 20 %. However there has been limited progress with blue emission compared to the red and green counterparts. In this review, the current status and challenges of blue PeLEDs are introduced, and strategies to produce spectrally stable blue PeLEDs are discussed. The strategies include 1) a mixed halide system in the form of 3-dimensional (3D) perovskites, 2) colloidal perovskite nanocrystals and 3) low dimensional perovskites, known as quasi-2D perovskites. In the mixed halide system, previous reports based on the compositional engineering of 3D perovskites to reduce spectral instability (i.e., halide segregation) will be discussed. Since spectral instability issue originate from the mixed halide composition in perovskites, the two other strategies are based on enlarging the band gap with a single halide composition. Finally, the prospects for each strategy are discussed, for further improvement in spectrally stable blue PeLEDs.

Key words halide perovskites, blue LEDs, mixed halide, dimensional engineering, perovskite nanocrystals.

1. Introduction

Halide perovskites have a crystal structure of ABX_3 (A^+ = $CH_3NH_3^+$ (MA^+), $CH(NH_2)_2^+$ (FA^+), Cs^+; B^{2+} = Pb^{2+}, Sn^{2+}; X = halides ions, Cl^-, Br^-, I^-) and show superior optoelectronic properties such as high carrier mobility,[1] long exciton diffusion length,[2] high absorption coefficient,[3] and largely tunable emission wavelengths.[4] Those properties are most suitable for not only for solar cell application but also for light emitting diodes (LEDs) thanks to their narrow emission linewidth, and highly tunable emission wavelengths from ultra-violet (UV) to near-infrared (NIR). The first perovskite LED (PeLED) that operates at room temperature was demonstrated by Tan et al., in 2014,[5] with relatively modest device external quantum efficiency (EQE) of 0.76 % (NIR), 0.1 % (red) and 0.018 % (green). Ever since rapid progress in device EQE has been shown with the current record EQEs over 20 % in NIR,[6-9] red,[10-12] and green PeLEDs.[13-16] The progress in EQE of PeLED has been realized through compositional engineering, dimensional engineering and developments in better synthesis protocol of perovskite nanocrystals (NCs), as well as engineering in device structures. However, in blue PeLEDs, a crucial component for displays and lighting, show limited progress compared to red and green till now. In this review, we classify the strategies to produce blue PeLEDs into three categories, including defect passivation in mixed halide perovskites, dimensional engineering by forming 2D or quasi-2D perovskites, and perovskite nanocrystals. The current status and challenges in blue PeLEDs, strategies that have been proposed to overcome the challenges will be discussed in the following sections.

†Corresponding author
E-Mail : byungha@kaist.ac.kr (B. Shin, KAIST)

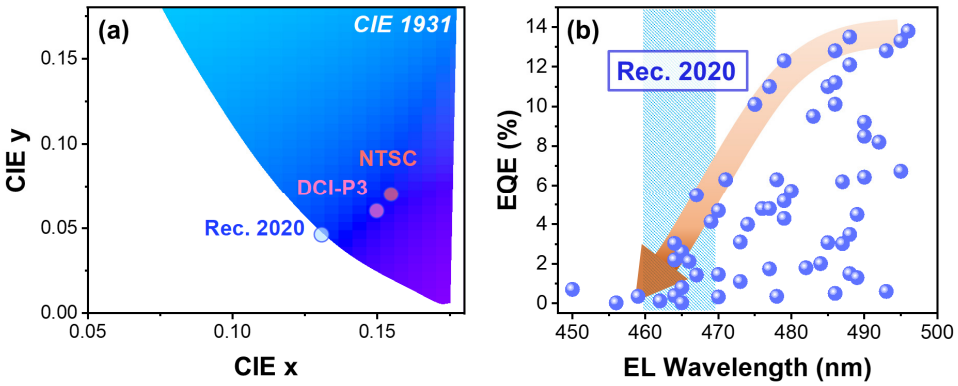

Fig. 1. (a) Shift in CIE coordinates of primary color of blue in display industries as technology develops, (b) trends in external quantum efficiency (EQE) vs electroluminescence (EL) wavelength of reported blue perovskite LEDs.

2. Current Status and Challenges in Blue PeLEDs

As the display technology develops, the demand for high-resolution displays that can express natural colors in high fidelity is growing. As a standard for UHDTV, Rec. 2020 has been proposed, which aims to cover 75.8 % of the CIE 1931 color space with three primary colors. The CIE coordinate of primary blue in Rec. 2020 is located at (0.131, 0.046), corresponding to the emission wavelength of 467 nm, which locates much closer to an edge of the color space compared to NTSC or DCI-P3 standards [Fig. 1(a)]. As the emission linewidth becomes narrower, the CIE coordinate is expressed closer to the edge of the color space. Blue LEDs which can produce an emission wavelength close to 467 nm with narrow linewidth is under critical demand in the display technology.

However, the emission wavelengths of reported blue PeLEDs with high EQE over 10 % were mostly above 480 nm, which is far from the requirement of Rec. 2020 standard [Fig. 1(b)]. EQE values of the reported PeLEDs gradually decrease as the emission wavelength decreases, and the highest EQE was below 6 % at the emission wavelength matches to Rec. 2020 standard (emission wavelength in the range of 460 nm to 470 nm).

A most convenient way to tune the band gap of perovskite is tuning the halide composition by mixing bromine and chlorine for blue emission. Since chlorine ions are smaller than bromine ions, the lattice constant of perovskite decreases as the content of chlorine increases, leading to widening of band gap of perovskite (Fig. 2).[4)]

However, spectral instability, in which electrical bias causes a shift in electroluminescence (EL) wavelength, is one of the main challenging issues in mixed halide PeLEDs.[17,18)] The

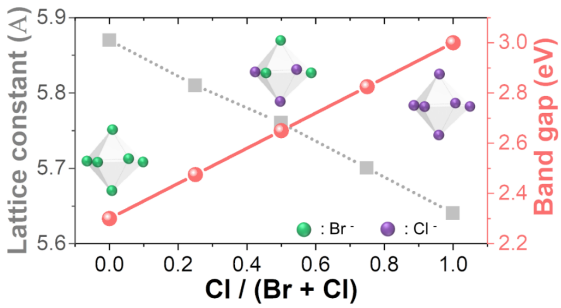

Fig. 2. Change in lattice constant in $CsPb(Br,Cl)_3$ perovskites with respect to different halide compositions. The band gap linearly increases as the ratio of Cl increases.

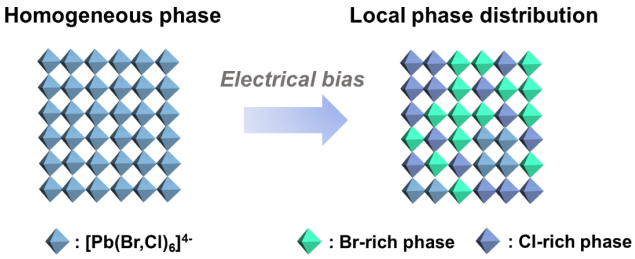

Fig. 3. Schematic illustration of halide segregation in mixed halide perovskites upon electrical bias (LED operation).

spectral instability issue arises by the formation of local phase separation due to halide segregation in mixed halide perovskite films caused by electric field driven halide ion migration (Fig. 3).

Halide perovskite has an inherent ionic crystal nature, and halide ion migration seems inevitable because the activation energy of halide ion migration is relatively low, compared to A-site cations or lead cations.[19-22)] Halide ions have negative charge, therefore the electric field applied during EL device operation can accelerate the migration of halides and induce

the spectral instability. The main route for the migration of mobile ions is reported to be defect sites, as well as grain boundaries. Reduction of defects and passivation of grain boundaries through compositional engineering in perovskite therefore can be an effective way to greatly reduce color instability issue in mixed halide perovskites. Another way to circumvent the spectral instability issue is tuning bandgap while maintaining a single bromide composition. The first option is quantum confinement—formation of colloidal nanocrystals smaller than Bohr radii to enlarge band gap. Another option is dimensional reduction of perovskite lattice, by construction of 2D or quasi-2D structures using bulky ammonium cations which act as a spacer separating layers of [PbX_6] octahedra.

In the following sections, we will discuss three approaches to produce spectrally stable blue PeLEDs; i) compositional engineering in mixed-halides, ii) single bromide perovskite nanocrystals with their size under Bohr radii, and iii) dimensional engineering of perovskites in single bromide compositions (Fig. 4).

3. Strategies for Spectrally Stable Blue PeLEDs

3.1. Compositional engineering in mixed halide system

The first 3D, mixed halide blue PeLEDs was demonstrated in 2015 by Kumawat et al.,[23] using $MAPb(Br_{1-x}Cl_x)_3$ thin films. The reported LED performance was rather low: EQE of ~10^{-4} % and luminance of 2 cd/m^2 due to poor film morphology. Wang et al.[24] succeeded in producing dense films by increasing a molar ratio of MA^+ while decreasing overall concentration of precursor solutions. With this approach they demonstrated sky-blue PeLEDs at 490 nm with a high luminance of 154 cd/m^2. Using multiple cations have been also effective way to improve film morphology.[25,26]

Enhancement in EQE as well as spectral stability were achieved in sky-blue region; however, for pure-blue emission in the range of 460 - 470 nm, Cl ions needed to be incorporated to further blueshift the emission. Realizing pure-blue emission by increasing Cl-containing precursor salts is not technically easy. For example, organic ammonium chlorides, such as MACl are highly hygroscopic and become easily evaporated during film formation, forming a high density of structural defects.[27] The inorganic chlorides, such as CsCl and $PbCl_2$, are free from the volatility issue, however their low solubility in common precursor solvents (i.e. DMF and/or DMSO) makes it difficult to increase Cl content above a certain limit in perovskite films.[28] Defects within perovskite film not only lower photoluminescence quantum yield (PLQY) but also lead to significant spectral stability issue during device operation. To solve these issues the introduction of RbX (X = Br, and Cl) was proposed.[28] Since Rb^+ (161 pm) has a smaller ion radius than Cs^+ (174 pm), the partially substituted Rb^+ induces the shrinkage of perovskite lattice, leads to band gap enlargement. Incorporation of RbCl brings about synergetic effects of shrinking lattice spacings as well as allowing a large incorporation of Cl, which leads to the shift of EL wave-

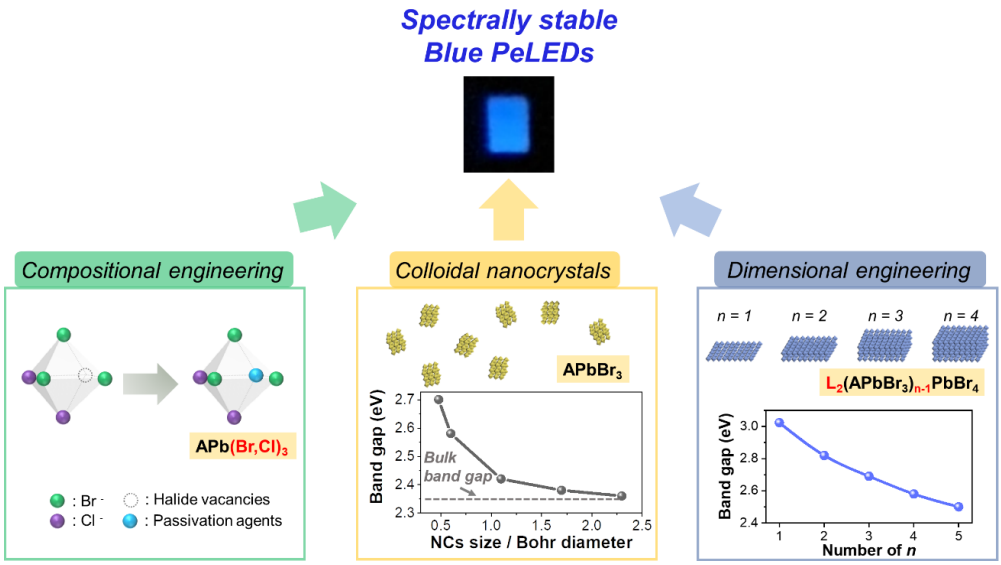

Fig. 4. Schematic illustration of three approaches for producing spectrally stable blue PeLEDs.

length to 468 nm with improved spectral stability. EQE was modest at 0.062 %, mainly due to a low PLQY (~0.25 %) of the emitter.

In order to reduce defect density, Wang et al. added phenethylammonium chloride (PEACl) and YCl_3 into precursor solutions.[29] Incorporation of PEACl and YCl_3 helps increase the activation of ion migration, and YCl_3 simultaneously acts as a passivation layer for grain boundaries of perovskite. The approach led to impressive EQE of 11 % at 487 nm, with maximum luminance of 9048 cd/m^2. Ma et al. adopted a so-called chloride insertion-immobilization strategy, in which diphenylphosphinic chloride (DPPOCl) organic halide source was used as dopants.[30] DPPOCl in the precursor solution reacts with a residual water in DMSO and forms DPPOOH, and the halide ions strongly bind to phosphoryl group of DPPOOH, resulting in spectrally stable EL emission at 479 nm with high EQE of 5.2 %. Recently, impressive EQE of 11 % at 477 nm (40 % Cl ions) and EQE of 5.5 % at 467 nm (45 % Cl ions) were reported by Karlsson, M et al., via vapor-assisted crystallization (VAC) technique.[31] The role of VAC is rearranging halide components and homogenizing the local chemical compositions. The solubility of chloride and bromide compounds are quite different, therefore as-casted films are composed of locally Cl-rich and Br-rich regions. The VAC retards the crystallization of an as-casted film, and halide exchange occurs between Cl-rich and Br- rich phases induced by chemical potential difference, resulting in a homogeneous film. A VAC-treated film showed improved spectral stability compared to the control sample, but spectral instable region reappeared at high enough current densities, indicating the spectral stability issue was not perfectly resolved.

3.2. Colloidal nanocrystals in single halide system

The first pure bromide colloidal perovskite nanocrystals (PNCs) for blue light emitting diodes were reported by Kumar et al.[32] They prepared $MAPbBr_3$ NCs by ligand assisted re-precipitation method and fabricated blue PeLEDs at wavelength of 456 nm with EQE_{max} of 0.0058 % and luminance of 1.4 cd/m^2. The device performance was low but as anticipated there was no issue of spectral instability because the system was based on pure bromide. PNCs are generally synthesized with long organic ligands but in order to improve charge transport and increase QD coupling it is better to replace long ligands with shorter ligands. The ligand exchange of PNCs is normally conducted in a polar solvent but this can lead to the decomposition of highly ionic perovskite NCs. Dong et al.[33] attempted to overcome this issue by adding isopropylammonium bromide (IPABr) to the colloidal solution to form an 'anion inner shell'. This approach improved the carrier mobility ($\geq$ 0.01 cm^2 V^{-1} s^{-1}) of the perovskite NCs and reduced a trap density, resulting in a blue-emitting film with a PLQY exceeding 90 %. PeLEDs based on $CsPbBr_3$ NCs showed an EQE of 12.3 % with luminance of ~270 cd/m^2 at an emission wavelength of 479 nm. Bi et al.[34] etched the uncoordinated $[PbBr_6]^{4-}$ octahedra using hydrogen bromide with didodecylamine and phenethylamine molecules, which removed surface defects and excess carboxylate groups. These additives bound to residual non-coordinating region of NC surfaces, and a PLQY of 97 % and high stability were demonstrated. This strategy showed high luminance of 3850 cd/m^2 with EQE of 4.7 % at 470 nm. Furthermore, the device exhibited excellent stability with a half-lifetime exceeding 12 h under continuous operation. Deep-blue emitting $CsPbBr_3$ NCs have a deep ionization potential ($\geq$6.5 eV), therefore they have a poor electrical interface with a hole transport layer. Hoye et al.[35] applied a poly(triarylamine) interlayer between a hole transport layer and a perovskite layer to reduce non-radiative recombination at the interface, achieving EQE of 0.3 % with peak luminance of 40 cd/m^2 at 464 nm. Yin et al.[36] introduced polyethylenimine (PEI) into $CsPbBr_3$ NCs to prevent coalescence between NCs. The approach led to a reduced defect density such as Br vacancies and improved stability. The short length of PEI ligand also reduced the distance between NCs and increased carrier hopping and tunneling between them. PeLED based on ligand exchanged $CsPbBr_3$ NCs exhibited peak luminance of 631 cd/m^2 with EQE 0.8 % at peak wavelength of 465 nm.

3.3. Dimensional engineering in single halide system

Quasi-2D perovskite (namely as Ruddlesden-Popper perovskite, RPP), with the chemical formula of $L_2(APbX_3)_{n-1}PbX_4$ (L: bulky ammonium cation; A = MA^+, FA^+, Cs^+; X = Cl^-, Br^-, I^-) shows a promising feature for LED application, such as high exciton binding energy, higher radiative recombination rate and higher stability, when compared to 3D counterparts.[37,38] The value of n represents the number of

lead halide octahedron sheets that is connected along z-axis [Fig. 5(a)]. The interesting feature of the quasi-2D perovskite is that the band gap is largely tunable with different *n* values [Fig. 5(b)].

While forming quasi-2D structure allows to enlarge band gap using pure bromide composition without mixing different kinds of halide, however, a quasi-2D film prepared by a stoichiometric ratio of precursor chemicals generally contains multiple phases with different *n* values.[39-44] The undesirable formation of multiple phases within quasi-2D perovskite films leads to the deviation of emission wavelength from a target value due to energy funneling process where electron-hole pairs injected to lower *n* (i.e., larger band gap) phase tend to migrate to the highest *n* phase (i.e., the smallest band gap).[39-44] Therefore, achieving uniform phase is essential to realize pure blue PeLEDs using quasi-2D films. In this section, strategies to synthesize single bromide quasi-2D films without formation of high *n* phases ($n > 3$, for pure blue emission) will be discussed.

To make narrow phase distribution within quasi-2D film, Liu et al. controlled the crystallization rate by adding an off-stoichiometric ratio of phenylbutylammonium (PBA) cations. Excess PBA cations were washed out using ethyl acetate during anti-solvent dripping.[45] The resultant film showed unique film configuration in which $Cs_xFA_{1-x}PbBr_3$ NCs were imbedded in a quasi-2D perovskite film. By increasing the ratio of PBABr in the precursor solution, the size of $Cs_xFA_{1-x}PbBr_3$ NCs was reduced, resulting in blueshift of the emission wavelength from 494 nm to 474 nm (but a secondary peak at 440 nm coexisted). The device showed an impressive EQE of 9.5 %, with a maximum luminance of 700 cd/m^2 at 483 nm. Xing et al. found that strong Van der Waals interaction between phenethylammonium (PEA) cations facilitates the formation of $n = 1$ phase at the earlier stage of film formation. They further explained that depeletion of PEA cations in the early stage forming the $n = 1$ phase leads to the formation of $n = \infty$ (3D) phase.[46] The authors substituted PEA cations with iso-propylammonium (IPA) to weaken the interaction between PEA cations, and as a result, the phase distribution of the film changed from the dominance of $n = 1$ and $n = \infty$ to $n = 2, 3, 4$. However, the final device showed sky-blue emission at 490 nm (EQE = 1.5 %), which deviates from the pure-blue emission region. In a similar approach, Yuan et al., used 1,4-Bis(aminomethyl)benzene bromide (P-PDABr$_2$) and PEABr as bulky ammonium ligands.[47] Through the optimization of the ratio of P-PDABr$_2$ to PEABr in a precursor solution, they synthesized films with a narrow phase distribution—only $n = 2$ and $n = 3$. EL devices produced pure-blue emission at 465 nm with EQE of 2.6 %. Wang et al.[48] proposed a chelating-agent-assisted control method, in which zwitterionic nature of Y-aminobutyric acid (GABA) additives helps not only passivate undercoordinated Pb atom but also suppress

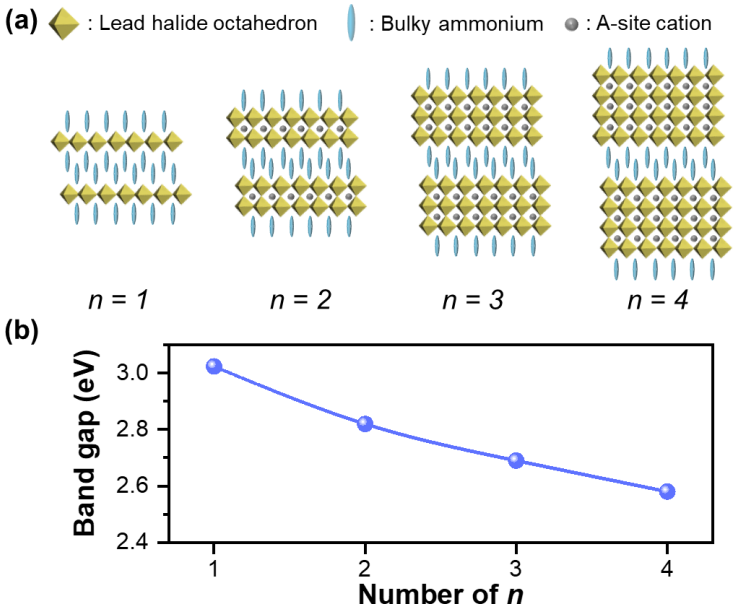

Fig. 5. (a) Crystal structure of Ruddlesden-popper perovskite (RPP) with different *n* values. (b) Theoretical band gap of RPP with different *n* value.

the formation of $n > 3$ phases. With this strategy, a high EQE of 6.3 % at 470 nm was demonstrated from EL devices.

Recently, Chen et al.[49] demonstrated, for the first time, blue PeLEDs based on single crystalline RPP, $(BA)_2Cs_{n-1}Pb_nBr_{3n+1}$ (n = 2 or n = 3). Free standing single crystalline RPP was grown in an aqueous HBr solution and a thin layer of the RPP was micro-mechanically exfoliated to serve as an emitting layer. PeLEDs based on n = 2 and n = 3 showed emission wavelengths of 450 nm and 482 nm, corresponding to the intrinsic band gap of RPP single crystals, with EQE of 0.7 % and 1.1 %, respectably. However, incomplete coverage of the emitter film with discontinuous morphology caused severe Joule heating and resulted in fast thermal degradation of the device.

4. Features and Prospects of Pure Blue Perovskite LEDs

The summary of aforementioned strategies for producing blue PeLED is listed in Table 1.

Relatively low exciton binding energy of 3D perovskites limits the performance of PeLED.[50] Additionally, chlorine must be introduced to a bromide-based 3D perovskite to enlarge a band gap large enough for blue emission. However, $PbCl_2$ has a low solubility in a common solvent used for perovskite precursor solutions. More importantly, mixed halide systems easily succumb to phase separation during operation, therefore the fabrication of high performing and stable PeLEDs in the deep blue region based on 3D perovskite still remains very challenge.

Colloidal perovskite NCs have higher stability against external stimuli such as water and oxygen thanks to the presence of long chain alkyl ligands on the surface. These ligands not only protect the NCs from the environments, but also leads to a high PLQY. Homogeneously sized NCs can be synthesized via precise control of the concentrations of synthetic precursors and ligands, and the luminescence spectra can be tuned over a wide range by utilizing the quantum confinement effect.[4] The composition of blue-emitting colloidal NCs of a carefully controlled dimension can be pure Br, which has superior spectral stability compared to NCs made of pure 3D perovskite of mixed anions (i.e., Br and Cl). In addition, the exciton binding energy can reach several hundred meV, which is much higher than that of pure 3D perovskite. In the case of perovskite NCs dispersed in solution, it has a PLQY reaching almost ~100 %.[51] Tightly bound excitons can promote the thermal stability of PeLEDs based on colloidal NCs by preventing exciton quenching due to high Joule heat generated during device operation. However, a NC system has drawbacks: 1) A PLQY of a film cased with colloidal NCs is lower than that of a suspension state. The reason for this deterioration is the loss of ligands which occurs during washing and film formation—this becomes more serious for smaller NCs with a larger surface/volume ratio. 2) The insulating nature of alkyl chains hinders charge injection into perovskite NCs degrading the EL device performance.

In order to solve the abovementioned issues, we propose the following research directions. 1) For tight binding between ligands and perovskite core, strategies such as post-treatment[10] or in-situ passivation[52] should be applied. 2) To increase the conductivity of a perovskite NC film, excess insulating ligand should be removed without degrading PLQY. Replacement of long ligands with those with a short chain

Table 1. Summary of three strategies for producing blue PeLED.

	Compositional engineering	Colloidal nanocrystals	Dimensional engineering
Way to tune the bandgap	Mixing halide compositions in ABX_3 lattices	Reduction of crystal size under Bohr radii	Construction of two-dimensional lattice: $L_2(APbX_3)_{n-1}PbX_4$
Advantages	- Easiest way to tune the bandgap - High carrier mobility	- High PLQY from passivation of surface ligands - Spectral stability (single halide)	- Spectral stability (single halide) - Higher stability compared to 3D counterpart
Disadvantages	- Spectral instability from halide segregation - Low PLQY due to low exciton binding energy	- Low charge mobility due to presence of surface ligands - Careful control of the crystal size is important	- Difficulties in regulating phase (n) distribution - Low charge mobility compared to 3D lattices

length should be performed.

Quasi-2D perovskite film has a larger exciton binding energy than 3D perovskite. Compared to colloidal perovskite NCs, a quasi-2D perovskite film can be formed directly from the precursor solution, avoiding an issue with the ligand loss which inevitably occurs during the purification process of colloidal NCs. The carbon chain length of the large molecules (e.g. phenethylamine) separating sheets of octahera in quasi-2D is much shorter than ligands (e.g. oleic acid, oleylamine) commonly used for colloidal perovskite NCs, so carrier transport is in generally easier in quasi-2D than NCs.

Previous studies have shown that quasi-2D perovskites can be used as good light-emitting layers for blue-emitting PeLEDs.[48,53-58] However, in order to further improve device performance, the following problems must be solved. 1) Methods to better control of phase distribution to be closer to the single phase are needed.[59] In previous studies, the way to synthesize pure blue quasi-2D films without formation of $n > 3$ phases were main focus, so the films still possess phases distributions of n values with the combination of $n = 1$ to 3. Recent study on quasi-2D based LEDs have shown that certain amount of non-radiative recombination losses happens during the charge carriers funnel into a largest n domain (smallest band gap), lowering the device performance, as well as broadening in emission spectrum.[60] Therefore, the generation of unwanted domains degrades color purity as well as device performance. 2) Another problem is the low electrical conductivity of blue quasi-2D films. Adding an excess of bulk ammonium cations facilitates the formation of low n phases to produce blue emission. However, the electrically insulating natures of bulk ammonium cations hinder charge transfer across perovskite film, limit the brightness of quasi-2D PeLEDs compared to 3D counterparts. It is nearly impossible to simultaneously improve electrical conductivity, phase distribution and PLQY of quasi-2D perovskite only by controlling the concentration of bulk cations. Therefore, new approaches for regulating the n distribution during crystallization of the quasi-2D films without hindering electrical conductivity of quasi-2D films must be needed.

5. Conclusion

Rapid progress in device external quantum efficiency has been accomplished in NIR, red and green perovskite LEDs (PeLEDs), however, in blue, which is a key component for displays and lighting, shows relatively slower progress compared to red and green so far. One of the major challenging issues of blue PeLEDs is resolving spectral instability issues in mixed halide system, which comes from the movement of halide ions upon device operation, results in local phase distribution of halide components. Since the control of halide composition is the easiest way to tune the bandgap, many of the works have been reported the way to reduce spectral instability in mixed halide system. Alternatively, the ways to enlarge bandgap using single halide compositions have been proposed. In this review, we categorized the various methods that have been developed to produce spectrally stable blue PeLEDs into three strategies (i.e. compositional engineering in mixed halide, colloidal nanocrystals and dimensional engineering in single halide system). Each of the strategies has its own different pros and cons, and still has room for further development. Therefore, it is difficult to say which strategy is the most promising for highly efficient blue light-emitting perovskite LED, so the research should be conducted in diverse aspects. Additionally, for the bright future in blue PeLEDs, the device operational lifetime must be improved, which is quite lower than the lifetime of QLEDs or OLEDs.[61] Careful design of the device structures, passivation of defects which generate at the interfaces of adjacent layers of perovskites, and thermal management during operation should be conducted in the future, not only for the higher EQE, as well as prolonged device lifetime.

Acknowledgement

We would like to thank POONGSAN R&D INSTITUTE for their financial support for this research project in 2022.

References

1. C. Wehrenfennig, G. E. Eperon, M. B. Johnston, H. J. Snaith and L. M. Herz, Adv. Mater., **26**, 1584 (2014).
2. S. D. Stranks, G. E. Eperon, G. Grancini, C. Menelaou, M. J. P. Alcocer, T. Leijtens, L. M. Herz, A. Petrozza and H. J. Snaith, Science, **342**, 341 (2013).
3. Z. Xiao, Q. Dong, C. Bi, Y. Shao, Y. Yuan and J. Huang, Adv. Mater., **26**, 6503 (2014).
4. L. Protesescu, S. Yakunin, M. I. Bodnarchuk, F. Krieg, R. Caputo, C. H. Hendon, R. X. Yang, A. Walsh and M. V.

Kovalenko, Nano Lett., **15**, 3692 (2015).
5. Z.-K. Tan, R. S. Moghaddam, M. L. Lai, P. Docampo, R. Higler, F. Deschler, M. Price, A. Sadhanala, L. M. Pazos, D. Credgington, F. Hanusch, T. Bein, H. J. Snaith and R. H. Friend, Nat. Nanotechnol., **9**, 687 (2014).
6. X. Zhao and Z.-K. Tan, Nat. Photonics, **14**, 215 (2020).
7. W. Xu, Q. Hu, S. Bai, C. Bao, Y. Miao, Z. Yuan, T. Borzda, A. J. Barker, E. Tyukalova, Z. Hu, M. Kawecki, H. Wang, Z. Yan, X. Liu, X. Shi, K. Uvdal, M. Fahlman, W. Zhang, M. Duchamp, J.-M. Liu, A. Petrozza, J. Wang, L.-M. Liu, W. Huang and F. Gao, Nat. Photonics, **13**, 418 (2019).
8. Y. Cao, N. Wang, H. Tian, J. Guo, Y. Wei, H. Chen, Y. Miao, W. Zou, K. Pan, Y. He, H. Cao, Y. Ke, M. Xu, Y. Wang, M. Yang, K. Du, Z. Fu, D. Kong, D. Dai, Y. Jin, G. Li, H. Li, Q. Peng, J. Wang and W. Huang, Nature, **562**, 249 (2018).
9. Y. Miao, L. Cheng, W. Zou, L. Gu, J. Zhang, Q. Guo, Q. Peng, M. Xu, Y. He, S. Zhang, Y. Cao, R. Li, N. Wang, W. Huang and J. Wang, Light Sci. Appl., **9**, 89 (2020).
10. Y. Hassan, J. H. Park, M. L. Crawford, A. Sadhanala, J. Lee, J. C. Sadighian, E. Mosconi, R. Shivanna, E. Radicchi, M. Jeong, C. Yang, H. Choi, S. H. Park, M. H. Song, F. D. Angelis, C. Y. Wong, R. H. Friend, B. R. Lee and H. J. Snaith, Nature, **591**, 72 (2021).
11. T. Chiba, Y. Hayashi, H. Ebe, K. Hoshi, J. Sato, S. Sato, Y.-J. Pu, S. Ohisa and J. Kido, Nat. Photonics, **12**, 681 (2018).
12. Z. Fang, W. Chen, Y. Shi, J. Zhao, S. Chu, J. Zhang and Z. Xiao, Adv. Funct. Mater., **30**, 1909754 (2020).
13. Y. Shen, L. Cheng, Y. Li, W. Li, J. Chen, S. Lee and J. Tang, Adv. Mater., **31**, 1901517 (2019).
14. K. Lin, J. Xing, L. N. Quan, F. P. G. de Arquer, X. Gong, J. Lu, L. Xie, W. Zhao, D. Zhang, C. Yan, W. Li, X. Liu, Y. Lu, J. Kirman, E. H. Sargent, Q. Xiong and Z. Wei, Nature, **562**, 245 (2018).
15. Y. Jiang, M. Cui, S. Li, C. Sun, Y. Huang, J. Wei, L. Zhang, M. Lv, C. Qin, Y. Liu and M. Yuan, Nat. Commun., **12**, 336 (2021).
16. Y.-H. Kim, S. Kim, A. Kakekhani, J. Park, J. Park, Y.-H. Lee, H. Xu, S. Nagane, R. B. Wexler, D.-H. Kim, S. H. Jo, L. Martínez-Sarti, P. Tan, A. Sadhanala, G.-S. Park, Y.-W. Kim, B. Hu, H. J. Bolink, S. Yoo, R. H. Friend, A. M. Rappe and T.-W. Lee, Nat. Photonics, **15**, 148 (2021).
17. P. Vashishtha and J. E. Halpert, Chem. Mater., **29**, 5965 (2017).
18. G. Li, F. W. R. Rivarola, N. J. L. K. Davis, S. Bai, T. C. Jellicoe, F. de la Peña, S. Hou, C. Ducati, F. Gao, R. H. Friend, N. C. Greenham and Z. Tan, Adv. Mater., **28**, 3528 (2016).
19. Y. Yuan and J. Huang, Accounts Chem. Res., **49**, 286 (2016).
20. H. Cho, Y. Kim, C. Wolf, H. Lee and T. Lee, Adv. Mater., **30**, 1704587 (2018).
21. J. Haruyama, K. Sodeyama, L. Han and Y. Tateyama, J. Am. Chem. Soc., **137**, 10048 (2015).
22. J. Mizusaki, K. Arai and K. Fueki, Solid State Ionics, **11**, 203 (1983).
23. N. K. Kumawat, A. Dey, A. Kumar, S. P. Gopinathan, K. L. Narasimhan and D. Kabra, ACS Appl. Mater. Interfaces, **7**, 13119 (2015).
24. Z. Wang, T. Cheng, F. Wang, S. Dai and Z. Tan, Small, **12**, 4412 (2016).
25. H. P. Kim, J. Kim, B. S. Kim, H. Kim, J. Kim, Abd. R. bin M. Yusoff, J. Jang and M. K. Nazeeruddin, Adv. Opt. Mater., **5**, 1600920 (2017).
26. F. Yuan, C. Ran, L. Zhang, H. Dong, B. Jiao, X. Hou, J. Li and Z. Wu, ACS Energy Lett., **5**, 1062 (2020).
27. A. Sadhanala, S. Ahmad, B. Zhao, N. Giesbrecht, P. M. Pearce, F. Deschler, R. L. Z. Hoye, K. C. Gödel, T. Bein, P. Docampo, S. E. Dutton, M. F. L. D. Volder and R. H. Friend, Nano Lett., **15**, 6095 (2015).
28. H. Wang, X. Zhao, B. Zhang and Z. Xie, J. Mater. Chem. C, **7**, 5596 (2019).
29. Q. Wang, X. Wang, Z. Yang, N. Zhou, Y. Deng, J. Zhao, X. Xiao, P. Rudd, A. Moran, Y. Yan and J. Huang, Nat. Commun., **10**, 5633 (2019).
30. D. Ma, P. Todorović, S. Meshkat, M. I. Saidaminov, Y.-K. Wang, B. Chen, P. Li, B. Scheffel, R. Quintero-Bermudez, J. Z. Fan, Y. Dong, B. Sun, C. Xu, C. Zhou, Y. Hou, X. Li, Y. Kang, O. Voznyy, Z.-H. Lu, D. Ban and E. H. Sargent, J. Am. Chem. Soc., **142**, 5126 (2020).
31. M. Karlsson, Z. Yi, S. Reichert, X. Luo, W. Lin, Z. Zhang, C. Bao, R. Zhang, S. Bai, G. Zheng, P. Teng, L. Duan, Y. Lu, K. Zheng, T. Pullerits, C. Deibel, W. Xu, R. Friend and F. Gao, Nat. Commun., **12**, 361 (2021).
32. S. Kumar, J. Jagielski, S. Yakunin, P. Rice, Y.-C. Chiu, M. Wang, G. Nedelcu, Y. Kim, S. Lin, E. J. G. Santos, M. V. Kovalenko and C.-J. Shih, ACS Nano, **10**, 9720 (2016).
33. Y. Dong, Y.-K. Wang, F. Yuan, A. Johnston, Y. Liu, D. Ma, M.-J. Choi, B. Chen, M. Chekini, S.-W. Baek, L. K. Sagar, J. Fan, Y. Hou, M. Wu, S. Lee, B. Sun, S. Hoogland, R. Quintero-Bermudez, H. Ebe, P. Todorovic, F. Dinic, P. Li, H. T. Kung, M. I. Saidaminov, E. Kumacheva, E. Spiecker, L.-S. Liao, O. Voznyy, Z.-H. Lu and E. H. Sargent, Nat. Nanotechnol., **15**, 668 (2020).
34. C. Bi, Z. Yao, X. Sun, X. Wei, J. Wang and J. Tian, Adv. Mater., **33**, 2006722 (2021).
35. R. L. Z. Hoye, M.-L. Lai, M. Anaya, Y. Tong, K. Gałkowski, T. Doherty, W. Li, T. N. Huq, S. Mackowski, L. Polavarapu, J. Feldmann, J. L. MacManus-Driscoll, R. H. Friend, A. S.

Urban and S. D. Stranks, ACS Energy Lett., **4**, 1181 (2019).
36. W. Yin, M. Li, W. Dong, Z. Luo, Y. Li, J. Qian, J. Zhang, W. Zhang, Y. Zhang, S. V. Kershaw, X. Zhang, W. Zheng and A. L. Rogach, ACS Energy Lett., **6**, 477 (2021).
37. N. Wang, L. Cheng, R. Ge, S. Zhang, Y. Miao, W. Zou, C. Yi, Y. Sun, Y. Cao, R. Yang, Y. Wei, Q. Guo, Y. Ke, M. Yu, Y. Jin, Y. Liu, Q. Ding, D. Di, L. Yang, G. Xing, H. Tian, C. Jin, F. Gao, R. H. Friend, J. Wang and W. Huang, Nat. Photonics, **10**, 699 (2016).
38. J. Byun, H. Cho, C. Wolf, M. Jang, A. Sadhanala, R. H. Friend, H. Yang and T. Lee, Adv. Mater., **28**, 7515 (2016).
39. X. Yang, Z. Chu, J. Meng, Z. Yin, X. Zhang, J. Deng and J. You, J. Phys. Chem. Lett., **10**, 2892 (2019).
40. H. Tsai, C. Liu, E. Kinigstein, M. Li, S. Tretiak, M. Cotlet, X. Ma, X. Zhang and W. Nie, Adv. Sci., **7**, 1903202 (2020).
41. X. Yang, X. Zhang, J. Deng, Z. Chu, Q. Jiang, J. Meng, P. Wang, L. Zhang, Z. Yin and J. You, Nat. Commun., **9**, 570 (2018).
42. L. N. Quan, D. Ma, Y. Zhao, O. Voznyy, H. Yuan, E. Bladt, J. Pan, F. P. G. de Arquer, R. Sabatini, Z. Piontkowski, A.-H. Emwas, P. Todorović, R. Quintero-Bermudez, G. Walters, J. Z. Fan, M. Liu, H. Tan, M. I. Saidaminov, L. Gao, Y. Li, D. H. Anjum, N. Wei, J. Tang, D. W. McCamant, M. B. J. Roeffaers, S. Bals, J. Hofkens, O. M. Bakr, Z.-H. Lu and E. H. Sargent, Nat. Commun., **11**, 170 (2020).
43. S. Y. Lee, Y. S. Nam, J. C. Yu, S. Lee, E. D. Jung, S.-H. Kim, S. Lee, J.-Y. Kim and M. H. Song, ACS Appl. Mater. Interfaces, **11**, 39274 (2019).
44. Z. Wang, F. Wang, W. Sun, R. Ni, S. Hu, J. Liu, B. Zhang, A. Alsaed, T. Hayat and Z. Tan, Adv. Funct. Mater., **28**, 1804187 (2018).
45. Y. Liu, J. Cui, K. Du, H. Tian, Z. He, Q. Zhou, Z. Yang, Y. Deng, D. Chen, X. Zuo, Y. Ren, L. Wang, H. Zhu, B. Zhao, D. Di, J. Wang, R. H. Friend and Y. Jin, Nat. Photonics, **13**, 760 (2019).
46. J. Xing, Y. Zhao, M. Askerka, L. N. Quan, X. Gong, W. Zhao, J. Zhao, H. Tan, G. Long, L. Gao, Z. Yang, O. Voznyy, J. Tang, Z.-H. Lu, Q. Xiong and E. H. Sargent, Nat. Commun., **9**, 3541 (2018).
47. S. Yuan, Z. Wang, L. Xiao, C. Zhang, S. Yang, B. Chen, H. Ge, Q. Tian, Y. Jin and L. Liao, Adv. Mater., **31**, 1904319 (2019).
48. Y.-K. Wang, D. Ma, F. Yuan, K. Singh, J. M. Pina, A. Johnston, Y. Dong, C. Zhou, B. Chen, B. Sun, H. Ebe, J. Fan, M.-J. Sun, Y. Gao, Z.-H. Lu, O. Voznyy, L.-S. Liao and E. H. Sargent, Nat. Commun., **11**, 3674 (2020).
49. H. Chen, J. Lin, J. Kang, Q. Kong, D. Lu, J. Kang, M. Lai, L. N. Quan, Z. Lin, J. Jin, L. Wang, M. F. Toney and P. Yang, Sci. Adv., **6**, eaay4045 (2020).
50. T. C. Sum, S. Chen, G. Xing, X. Liu and B. Wu, Nanotechnology, **26**, 342001 (2015).
51. V. G. V. Dutt, S. Akhil, R. Singh, M. Palabathuni and N. Mishra, J. Phys. Chem. C, **126**, 9502 (2022).
52. Y. Wu, C. Wei, X. Li, Y. Li, S. Qiu, W. Shen, B. Cai, Z. Sun, D. Yang, Z. Deng and H. Zeng, ACS Energy Lett., **3**, 2030 (2018).
53. N. Yantara, N. F. Jamaludin, B. Febriansyah, D. Giovanni, A. Bruno, C. Soci, T. C. Sum, S. Mhaisalkar and N. Mathews, ACS Energy Lett., **5**, 1593 (2020).
54. P. Pang, G. Jin, C. Liang, B. Wang, W. Xiang, D. Zhang, J. Xu, W. Hong, Z. Xiao, L. Wang, G. Xing, J. Chen and D. Ma, ACS Nano, **14**, 11420 (2020).
55. Y. Liu, Z. Yu, S. Chen, J. H. Park, E. D. Jung, S. Lee, K. Kang, S.-J. Ko, J. Lim, M. H. Song, B. Xu, H. J. Snaith, S. H. Park and B. R. Lee, Nano Energy, **80**, 105511 (2021).
56. S. Yuan, L. Cui, L. Dai, Y. Liu, Q. Liu, Y. Sun, F. Auras, M. Anaya, X. Zheng, E. Ruggeri, Y. Yu, Y. Qu, M. Abdi-Jalebi, O. M. Bakr, Z. Wang, S. D. Stranks, N. C. Greenham, L. Liao and R. H. Friend, Adv. Mater., **33**, 2103640 (2021).
57. Z. Ren, J. Yu, Z. Qin, J. Wang, J. Sun, C. C. S. Chan, S. Ding, K. Wang, R. Chen, K. S. Wong, X. Lu, W. Yin and W. C. H. Choy, Adv. Mater., **33**, 2005570 (2021).
58. Y. Tian, X.-Y. Qian, C.-C. Qin, M.-H. Cui, Y.-Q. Li, Y.-C. Ye, J.-K. Wang, W.-J. Wang and J.-X. Tang, Chem. Eng. J., **415**, 129088 (2021).
59. H. Zhang, W. Li, X. Zhang, C. Yu, T. Li, X. Zhang, Z. Gao, C. Xiong and T. Wang, Appl. Phys. Lett., **118**, 083302 (2021).
60. D. Ma, K. Lin, Y. Dong, H. Choubisa, A. H. Proppe, D. Wu, Y.-K. Wang, B. Chen, P. Li, J. Z. Fan, F. Yuan, A. Johnston, Y. Liu, Y. Kang, Z.-H. Lu, Z. Wei and E. H. Sargent, Nature, **599**, 594 (2021).
61. F. Ye, Q. Shan, H. Zeng and W. C. H. Choy, ACS Energy Lett., **6**, 3114 (2021).

Author Information

Joonyun Kim
Ph.D. Candidate, Korea Advanced Institute of Science and Technology

Jinu Park
Ph.D. Candidate, Korea Advanced Institute of Science and Technology

Byungha Shin
Associate Professor, Korea Advanced Institute of Science and Technology